An Active 20-MHz to 2.5-GHz UWB Receiver Antenna System Using a TEM Horn

Mohammad Ali Salari, Omid Manoochehri, Amin Darvazehban, and Danilo Erricolo

***Abstract*—An ultrawideband receiver antenna system is proposed. The radiating element is a transverse electromagnetic horn antenna, featuring a negative impedance converter at lower frequencies. The voltage standing-wave ratio (VSWR) is less than 2.0 in the bandwidth from 20 MHz to 2.5 GHz. A good agreement between the measurements of the fabricated system and the simulated results is observed. Sample applications include direction finding, broadband communication systems, radar systems, and electromagnetic compatibility measurement systems.**

***Index Terms*—Broadband communications, direction finding, horn antenna, microstrip balun, negative impedance converter (NIC), radar system, ultrawideband (UWB).**

I. Introduction

WE PROPOSE an ultrawideband (UWB) receiver antenna system that maximizes its operational bandwidth to cover a huge number of bands from 20 MHz to 2.5 GHz. Its design was mainly motivated by a direction-finding application [1]–[3] where the goal was to replace three different narrowband antenna systems with a more compact UWB single-antenna system. Hence, benefits of the new design include: 1) a smaller physical size that results from replacing a 2-m monopole antenna with a horn antenna about 5 times smaller in its larger dimension; 2) using a single antenna instead of three; and 3), reducing the cost of the system. Many of these antenna systems may be used also in array configurations. Additional sample applications include radar systems [4], broadband communication systems [5], and electromagnetic compatibility (EMC) measurement systems.

In the case of direction-finding applications, a transverse electromagnetic (TEM) horn antenna is a suitable candidate for both its directivity and wideband behavior. However, the frequency at which a TEM horn starts to radiate efficiently is not sufficiently low. Therefore, our approach consists of dividing the overall operational bandwidth into two frequency ranges, as shown in the block diagram of Fig. 1. An RF switch is used to select between low and high frequencies. At low frequency, a negative impedance converter (NIC) is introduced to cancel the capacitive impedance of the antenna. At high frequency, an impedance matching network is used.

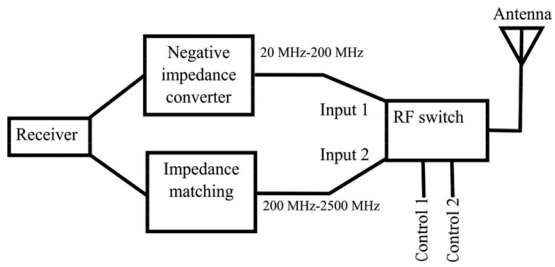

Fig. 1. Block diagram of the proposed antenna system. The RF switch is controlled by using control pins (control 1 and control 2) in order to select between low and high frequencies.

TABLE I
Comparison to Other Works

	Radiating Element	Frequency Range (MHz); Fractional Bandwidth (I)	$\lvert S_{11}\rvert$ (dB) (II)	# of Antennas (III)
This paper	Active TEM horn	20–2500; 1.97	$\mathrm{Min} = 10\,\mathrm{Max} = 33$	1
[6]	Conical dipole	20–1300; 1.94	$\mathrm{Min} = 1\,\mathrm{Max} = 18$	2
[7]	Conformal shaped dipoles	240–3300; 1.73	$\mathrm{Min} = 10\,\mathrm{Max} = 35$	2
[8]	Microstrip TEM horn	150–3000; 1.81	$\mathrm{Min} = 2\,\mathrm{Max} = 10$	2

Obviously, this approach can be extended to more than two frequency ranges. The TEM horn antenna as well as the NIC circuit are fabricated, and the results of the measurements are reported in the following. Table I compares some parameters of the present work to similar works to the best of the knowledge of the authors [6]–[8]. As can be seen, the proposed antenna system has the following advantages: 1) it has the largest fractional bandwidth thanks to the active matching circuit; 2) it has both a very wide bandwidth and a good return loss; 3) only one antenna is used to cover the whole operational bandwidth, unlike the others. As a result, the proposed system is simpler, smaller, cheaper, and lighter.

II. Antenna and NIC Design

A. TEM Horn

TEM horn antennas have been widely used in ground penetrating radar (GPR), EMC measurement systems, and broadband

Manuscript received April 28, 2017; revised June 12, 2017; accepted June 28, 2017. Date of publication July 4, 2017; date of current version August 21, 2017. *(Corresponding author: Mohammad Ali Salari.)*

M. A. Salari is with the Department of Physics, RWTH-Aachen University, Aachen 52074, Germany (e-mail: salari.mohammadali@gmail.com).

O. Manoochehri and D. Erricolo are with the Department of Electrical and Computer Engineering, University of Illinois at Chicago, Chicago, IL 60607 USA (e-mail: omanoo2@uic.edu).

A. Darvazehban is with the Department of Electrical Engineering, Amirkabir University of Technology, Tehran 159163-4311, Iran (e-mail: derric1@uic.edu).

Color versions of one or more of the figures in this letter are available online at http://ieeexplore.ieee.org.

Digital Object Identifier 10.1109/LAWP.2017.2723318

Fig. 2. (a) Dimensional parameters of the TEM horn antenna. At the aperture, we have $L = 300$ mm, $w = 243$ mm, and $d = 429$ mm. (b) Fabricated TEM horn.

communication systems [9]. Low distortion of pulse transmission, directional radiation pattern, low cross polarization, and wide bandwidth are some of the properties that make TEM horn antennas interesting for various applications [9], [10]. Various attempts have been made to improve the radiation characteristics of these antennas. Partial dielectric loading [11] and using TEM horn antenna with an inductive loop antenna for low-frequency radars [12] are among the methods to improve the intensity of the pulse radiation for GPR applications. A wider bandwidth can be achieved by shaping the antenna profile using an exponential [13] or even an elliptical [14] taper. In our design, an exponential taper is employed to match the characteristic impedance at the feed point to the impedance of free space. The gradual exponential transition keeps the reflections low and makes the bandwidth wider.

The antenna consists of two parts: 1) the horn section, and 2) the balun for matching the impedance of the TEM horn antenna with a balanced structure to an unbalanced coax feedline [10], [15]. Design parameters for the horn antenna with exponential taper are shown in Fig. 2(a), and (b) shows the fabricated horn antenna. The separation *d(y)* between the two plates of an exponentially tapered TEM horn antenna is given by [16]

$$d(y) = 2\left\{ae^{by}\right\}, \quad (0 \le y \le L) \tag{1}$$

where a and b are arbitrary coefficients to be determined. The characteristic impedance at any point on the antenna is expressed as [16]

$$Z(y) = Z_0 e^{\alpha y}, \quad (0 \le y \le L), \quad \alpha = \frac{1}{L} ln\left(\frac{Z_L}{Z_0}\right) \tag{2}$$

where $Z_0 = 50\ \Omega$, $Z_L = 120\pi\ \Omega$, and L is the antenna length. To determine the plate width, the characteristic impedance of a parallel-plate waveguide is employed, where the characteristic impedance between two plates is given by [14]

$$Z(y) = 120\pi \frac{d(y)}{w(y)} \tag{3}$$

and $w(y)$ is the plate width. The microstrip-type balun [16] to connect the coaxial feed to the antenna is shown in Fig. 3, and the corresponding values of the design parameters are given in Table II.

An alternative for the microstrip feed is to use a coax with an elliptical-shaped cavity in order to reduce reflections in the coaxial-to-double-ridged-waveguide transition [16]. However, according to our requirements, a microstrip balun is more suitable because it has smaller dimensions. As shown in Fig. 3, the width of the upper plate has an increasing taper, whereas the width of the ground plane has a decreasing taper such that a transition from the characteristic impedance of the coaxial line to that of the balanced parallel plates is obtained [10]. Unlike the balun proposed in [10], which uses a linear taper, additional optimized tapered sections are used in our design to improve the high-frequency performance of the balun. We should also note that the input impedance of the TEM horn antenna must be matched to the output impedance of the balun. Fig. 4 shows the simulated radiation pattern with CST [17] and the measured radiation pattern at various frequencies for the single TEM horn antenna with microstrip balun. As expected, for direction-finding applications, this antenna should be used in an array configuration. The radiation pattern of the antenna is almost omnidirectional at the lower frequencies. However, the beamwidth gets narrower as the frequency increases, but there

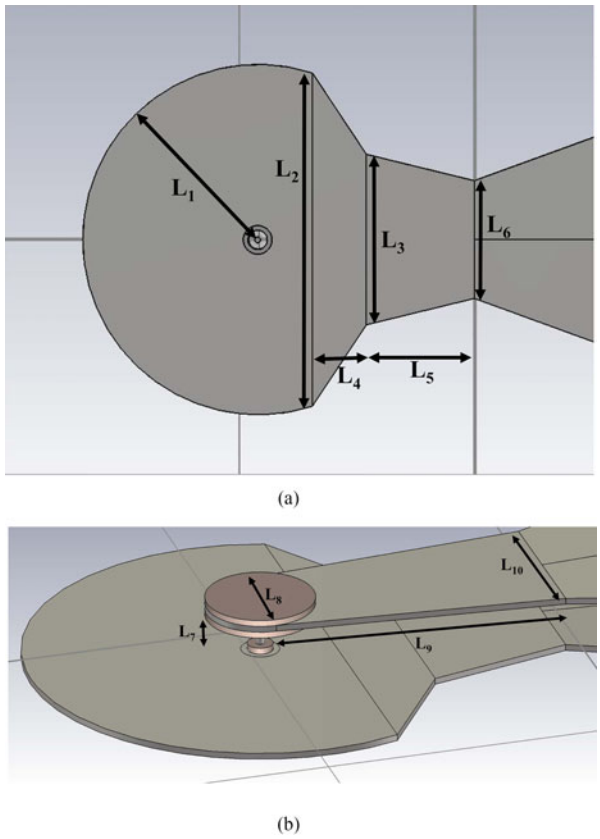

Fig. 3. Dimensions of the microstrip balun (a) bottom view, (b) top view. The discs with diameter L_8 provide mechanical support.

TABLE II
DIMENSIONS OF THE MICROSTRIP BALUN

Parameter	L_1	L_2	L_3	L_4	L_5
Value (mm)	**38**	**71**	**36**	**11.5**	**23**
Parameter	$\mathbf{L_6}$	$\mathbf{L_7}$	$\mathbf{L_8}$	$\mathbf{L_9}$	$\mathbf{L_{10}}$
Value (mm)	**25**	**7**	**17**	**46**	**25**

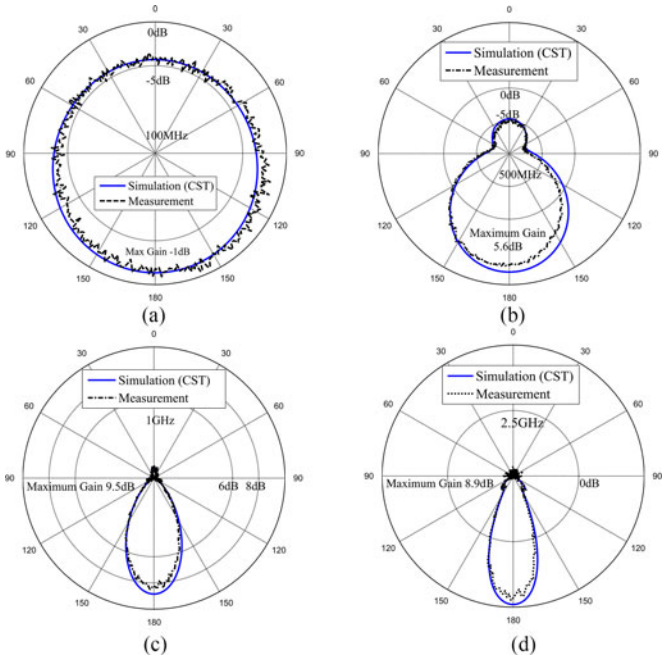

Fig. 4. Simulated and measured radiation pattern generated by the TEM horn antenna in the *xy* plane [see Fig. 2(a)] at (a) 100 MHz, (b) 500 MHz, (c) 1 GHz, and (d) 2.5 GHz.

exists a 3-dB beam overlap to cover the azimuth plane. It is worth mentioning that at each frequency, sampling algorithm in the software should be calibrated to decrease the errors due to the variations of the power magnitude.

B. Negative Impedance Converter

For the lower range of frequencies, i.e., below 200 MHz, the antenna remains electrically small and consequently has a narrow bandwidth. For electrically small antennas, passive (Foster) matching cancels the reactive part of the antenna impedance over a very narrow bandwidth [18]. However, it is possible to cancel the reactive part of the antenna input impedance over a wide bandwidth with non-Foster elements, such as an NIC. The NIC is an active two-port network that inverts the impedance connected to the other port [19], and one realization was provided by Linville [20]. The schematic of our NIC is provided in Fig. 5, where two transistors are biased in the common emitter configurations and their bases are connected to form a feedback loop [18]. Capacitor C_7 is then connected between the two collector leads. The transistors are NPN BJTs (BFR92) with class-A-type biasing that increases the voltage gain and fulfills the condition for having a negative impedance.

The circuit is fabricated on FR-4 substrate with permittivity 4.3 and thickness of 1 mm. We should notice also that the active elements exhibit internal losses, noise, and bandwidth limitations [21]. Moreover, parasitic reactances must be considered when the circuit is laid out. Therefore, the manufacturer's *S*-parameter file for the transistor is used in our simulations with ADS [22]. The output port is connected to a 50-Ω load, and the values of the elements, especially the capacitor C_7 of

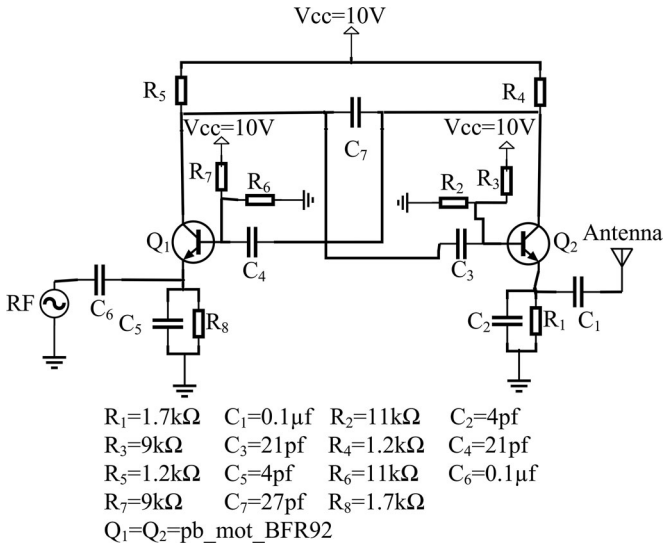

Fig. 5. Schematic of the NIC circuit. The values of the elements are also given.

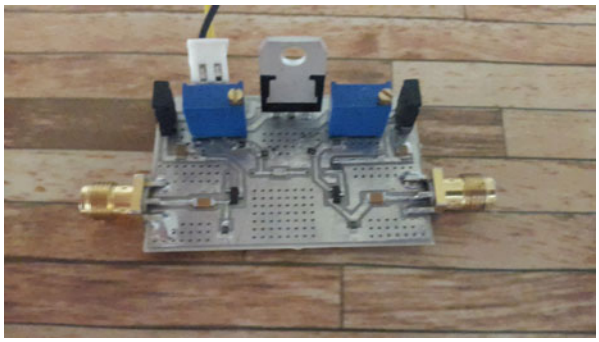

Fig. 6. Fabricated NIC circuit.

Fig. 5, are optimized to achieve an acceptable matching over the desired frequency band ($|S_{11}| < -10$ dB). Fig. 7(a) and (b) shows the real and imaginary parts of the input impedance as well as the reflection coefficient of the isolated antenna and the antenna connected to the NIC. As can be seen from Fig. 7(a), the NIC significantly reduces the large capacitive reactance of the antennas at low frequencies. Consequently, the real part of the impedance increases at low frequencies. The influence of the NIC can be observed also in the reflection coefficient in Fig. 7(c), where the simulation and measurement results are shown. The NIC significantly reduces the almost full reflection of the antenna at low frequencies as shown in Fig. 7(c). The insertion loss of NIC circuit varies between 2.9 and 4.6 dB over the frequency band from 20 to 200 MHz. An RF switch is introduced to bypass the NIC for frequencies above 200 MHz because of the excessive losses introduced by the NIC, as shown by the value of S_{11}. Above 200 MHz, the value of S_{11} of the antenna and NIC is below 10 dB, however, the losses are mostly due to the NIC losses and not radiation. The fabricated NIC circuit is shown in Fig. 6. As can be seen from the simulation and measurement results, the bandwidth of the whole system for voltage standing-wave ratio (VSWR) less than 2.0 is about 2.5 GHz (i.e., from 20 MHz to 2.5 GHz).

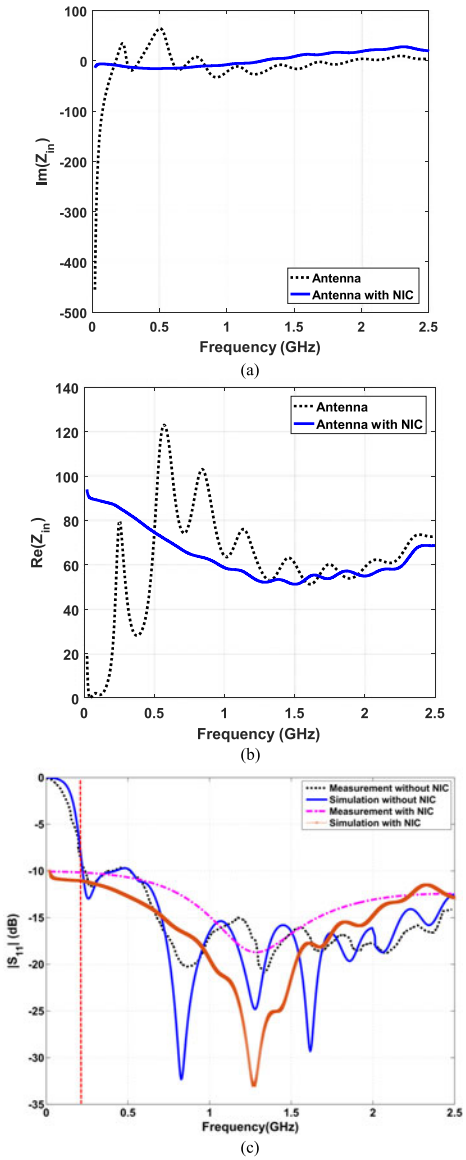

Fig. 7. (a) Imaginary part of the input impedance for the antenna with and without NIC. (b) Real part of the input impedance for the antenna with and without NIC. (c) *S*-parameter of the antenna without/with NIC.

III. Conclusion and Future Work

A UWB antenna system for the frequency range from 20 MHz to 2.5 GHz has been proposed. The operation bandwidth of the passive antenna is from 200 MHz to 2.5 GHz. An NIC circuit is used to reduce the capacitive behavior of the antenna from 20 to 200 MHz, which also improves the return loss. By using a simple RF switch in the antenna feed, the NIC can be switched in and out of the circuit. The insertion loss of NIC circuit varies between 2.9 and 4.6 dB over the frequency band from 20 to 200 MHz. This system has been simulated, optimized, fabricated, and measured. A good agreement between the measured and simulated results is observed. Future work will address the mutual coupling between the antennas in an array configuration.

References

[1] S. E. Lipsky, *Microwave Passive Direction Finding*, Raleigh, NC, USA: SciTech, 2004.
[2] R. Guinvarc'h, M. Serhir, and F. Boust, "A compact dual-polarized 3:1 bandwidth omnidirectional array of spiral antennas," *IEEE Antennas Wireless Propag. Lett.*, vol. 15, pp. 1909–1912, 2016.
[3] S. Ebihara, Y. Kimura, T. Shimomura, R. Uchimura, and H. Choshi, "Coaxial-fed circular dipole array antenna with ferrite loading for thin directional borehole radar sonde," *IEEE Trans. Geosci. Remote Sens.*, vol. 53, no. 4, pp. 1842–1854, Apr. 2015.
[4] J. P. Lie, C. M. See, and B. P. Ng, "Ultra wideband direction finding using digital channelization receiver architecture," *IEEE Commun. Lett.*, vol. 10, no. 2, pp. 85–87, Feb. 2006.
[5] R. Klukas and M. Fattouche, "Line-of-sight angle of arrival estimation in the outdoor multipath environment," *IEEE Trans. Veh. Technol.*, vol. 47, no. 1, pp. 342–351, Feb. 1998.
[6] C. Cho, I. Park, and H. Choo, "Design of a small antenna for wideband mobile direction finding systems," *Microw., Antennas Propag.*, vol. 4, no. 7, pp. 930–937, 2010.
[7] D. Caratelli, I. Liberal, and A. Yarovoy, "Design and full-wave analysis of conformal ultra-wideband radio direction finders," *Microw., Antennas Propag.*, vol. 5, no. 10, pp. 1164–1174, Jul. 2011.
[8] M. E. Ozturk, E. Korkmaz, and M. Kebeli, "Rounded-edge bow-tie antenna for wideband mobile direction finding system," *Microw., Antennas Propag.*, vol. 9, no. 15, pp. 1809–1815, Oct. 2015.
[9] K. Chung, S. Pyun, and J. Choi, "Design of an ultrawide-band TEM horn antenna with a microstrip-type balun," *IEEE Trans. Antennas Propag.*, vol. 53, no. 10, pp. 3410–3413, Oct. 2005.
[10] A. E. C. Tan, K. Jhamb, and K. Rambabu, "Design of transverse electromagnetic horn for concrete penetrating ultrawideband radar," *IEEE Trans. Antennas Propag.*, vol. 60, no. 4, pp. 1736–1743, Apr. 2012.
[11] A. Elsherbini and K. Sarabandi, "ENVELOP antenna: A class of very low profile UWB directive antennas for radar and communication diversity applications," *IEEE Trans. Antennas Propag.*, vol. 61, no. 3, pp. 1055–1062, Mar. 2013.
[12] T. C. Li-Chung and W. D. Burnside, "An ultrawide-bandwidth tapered resistive TEM horn antenna," *IEEE Trans. Antennas Propag.*, vol. 48, no. 12, pp. 1848–1857, Dec. 2000.
[13] S. Blume and B. Grafmuller, "Biconical antennas and conical horns with elliptic cross section," *IEEE Trans. Antennas Propag.*, vol. 36, no. 8, pp. 1066–1070, Aug. 1988.
[14] J. S. Mclean, R. Sutton, A. Medina, H. Foltz, and J. F. Li, "The Experimental characterization of UWB antennas via frequency-domain measurements," *IEEE Antennas Propag. Mag.*, vol. 49, no. 6, pp. 192–202, Dec. 2007.
[15] J. Shao, G. Fang, J. Fan, Y. Ji, and H. Yin, "TEM horn antenna loaded with absorbing material for GPR applications," *IEEE Antennas Wireless Propag. Lett.*, vol. 13, pp. 523–527, 2014.
[16] J. Church, J. C. S. Chieh, L. Xu, J. D. Rockway, and D. Arceo, "UHF Electrically small box cage loop antenna with an embedded non-foster load," *IEEE Antennas Wireless Propag. Lett.*, vol. 13, pp. 1329–1332, 2014.
[17] CST Microwave Studio, Version 2015, CST GmbH, Darmstadt, Germany.
[18] A. M. Elfrgani and R. G. Rojas, "Biomimetic antenna array using non-foster network to enhance directional sensitivity over broad frequency band," *IEEE Trans. Antennas Propag.*, vol. 64, no. 10, pp. 4297–4305, Oct. 2016.
[19] C. R. White, J. S. Colburn, and R. G. Nagele, "A Non-Foster VHF monopole antenna," *IEEE Antennas Wireless Propag. Lett.*, vol. 11, pp. 584–587, 2012.
[20] J. G. Linvill, "Transistor negative-impedance converters," *Proc. IRE*, vol. 41, no. 6, pp. 725–729, Jun. 1953.
[21] S. E. Sussman-Fort and R. M. Rudish, "Non-foster impedance matching of electrically-small antennas," *IEEE Trans. Antennas Propag.*, vol. 57, no. 8, pp. 2230–2241, Aug. 2009.
[22] Advanced Design System, Version 2016, Keysight Technologies, Inc., Santa Rosa, CA, USA, Aug. 2009.